

Hossein Moradi<sup>1,2</sup>, Saba Azima<sup>1\*</sup>, Reza Ebrahimi-Kahrizsangj<sup>2</sup>

<sup>1</sup> Islamic Azad University, Najafabad Branch, Department of Architecture, Najafabad, Iran

<sup>2</sup> Islamic Azad University, Najafabad Branch, Materials Engineering Department, Advanced Materials Research Center, Najafabad, Iran

\*Corresponding author. E-mail: saba.helix1375@gmail.com

Received (Otrzymano) 3.04.2023

## COMPARISON AND STUDY OF MECHANICAL AND PHYSICAL PROPERTIES OF METAKAOLIN REINFORCED GYPSUM COMPOSITE

This study investigated the effect of creating a composite of gypsum with metakaolin as well as the physical and mechanical behavior of the produced composites. For this purpose, gypsum composites were prepared with 2.9, 4.8, 6.5, and 9 wt.% metakaolin in 100 g of gypsum and a constant content of water. To determine the mechanical properties of the composites, the compressive strength test was used and the porosity, water absorption percentage, and bulk density of the composites were obtained using the Archimedes method. The results showed that the porosity was reduced by adding up to 7 wt.% metakaolin to the gypsum specimens, it increases the compressive strength by 41% and also raises the Young's modulus of gypsum by 121%. Scanning electron microscopy (SEM) equipped with energy-dispersive X-ray spectroscopy (EDS) was employed for the microstructural evaluations. The EDS-SEM observations showed the presence of Al and Si elements in the fracture zones. The presence of metakaolin elements at one point increases resistance in that area. Metakaolin-reinforced gypsum composites can be used in boards and panels.

**Keywords:** gypsum composite, metakaolin, mechanical behavior, compressive strength, Young's modulus

### INTRODUCTION

Gypsum is known as a semi-hydrated calcium sulfate [1]. This material has many applications as a building material due to its environmentally friendly and recyclable properties [2, 3], extensive resources, ease of use, and ease of production [4, 5]. Also, unique features such as good flexibility, heat, and sound insulation [6], beauty [7], and cost-effectiveness [8, 9] show that all the necessary conditions for expanding the scope of application of gypsum in the renovation and reconstruction of buildings are available [10]. Accordingly, the refurbishment of construction materials is focused on gypsum, gypsum-lime, and cement [11]. The main disadvantages of gypsum compared to materials such as cement and lime include low resistance to moisture, brittleness, and also low compressive strength, which restrict its application in some similar cases [12-16]. Plaster is primarily designed to protect load-bearing structures from environmental influences. At the same time, it must provide a building quality and beauty. Therefore, its durability is of vital importance for any structure or building [17]. Furthermore, because of its lightweight and fire resistance, gypsum is used on walls, ceilings, coatings, and in the reconstruction of old reliefs. Accordingly, many attempts have been made to overcome the weaknesses of gypsum through the use of additives [18, 19].

The effect of adding minerals and fibers to gypsum has been researched in various studies [1, 7, 20]. The results of these studies showed that the addition of these fibers can improve the mechanical properties, Young's modulus, and thermal resistance. In some other studies, synthetic fibers such as glass and textiles [16], plasticizers [21], pozzolanic additives, polymers [20], carbon nanotubes [22], and metakaolin [23, 24] have been used. In general, additives to gypsum mortar can improve its mechanical properties, especially cracking behavior [25, 26]. It also increases the compressive strength [10, 12, 13], flexural strength [15], tensile strength and adhesion [27], in addition to the flexibility [28] of the mortar.  $Al_2Si_2O_7$  or  $Al_2O_3 \cdot 2SiO_2$ , which is obtained from kaolinite at temperatures between 500 and 800°C, is mainly used as a cementation additive to replace Portland cement or to produce geopolymers [29]. One of the main drivers for the development of geopolymers is the desire to reduce greenhouse gas emissions. Some typical Australian raw material-based geopolymer concrete mix case studies show the potential to reduce greenhouse gas emissions by 44-64%, while the financial cost is 7% to 39% lower than OPC [30]. This claim is made only for the use of metakaolin only after it is used in the composite. Some published scientific LCA papers claim that in terms of CO<sub>2</sub>

emissions, geopolymers are not better than Portland cement, and worse for other parameters. The problem is that these values are taken for granted by other scientists without any further consideration of these cases: first, their present laboratory situation, second, the one that will prevail in 5-10 years from now when industrialization starts in full swing [31]. Metakaolin is an active amorphous aluminosilicate compound, the use of which improves the durability and refinement of pores in mortars or concretes [29]. Low strength limits the use of gypsum boards [20]; therefore, two of the topics studied in gypsum-based composites materials are their mechanical and physical behavior. Currently, there are few studies on metakaolin that can be used alone as a reinforcing agent in gypsum. Thus, this research is aimed at investigating the mechanical and physical behavior of a composite based on gypsum and metakaolin. The second purpose of this study is to present the behavior of different amounts of metakaolin in gypsum-based composites, based on which 4 groups of different weight percentages of metakaolin in gypsum are investigated.

## MATERIALS AND METHODS

### Materials

In this experiment, gypsum supplied by Salafchegan was used. The gypsum particle size distribution is presented in Table 1. Under the completely dry environment of the laboratory, 100 grams of pure powder was placed in a 5-layer wire mesh sieve device to measure the size distribution of particles above 10 microns. In this test, wire nets with dimensions of 1.7, 1.4, 0.3 and 0.106 mm were used.

TABLE 1. Particle size distribution of gypsum

wt. %	Particle size
0.20%	1.7 mm < x
0.64%	1.4 mm
7.80%	0.3 mm
47.15%	0.106 mm
44.15%	0.106 mm > x

The chemical composition was determined by X-ray fluorescence (XRF) analysis and is presented in Table 2. The percentage of calcium sulfate in this gypsum is higher than 85% and it can be used according to the ASTM C471M standard.

TABLE 2. Chemical composition of gypsum by XRF analysis [%]

Specimen	SiO <sub>2</sub>	Al <sub>2</sub> O <sub>3</sub>	Fe <sub>2</sub> O <sub>3</sub>	CaO	Na <sub>2</sub> O	MgO	K <sub>2</sub> O	TiO <sub>2</sub>	MnO	P <sub>2</sub> O <sub>5</sub>	LOI	SO <sub>3</sub>
WS	3.437	0.39	0.663	29.736	0.145	N	0.075	0.035	0.031	0.02	8.51	55.00

### Additives

The additive used is metakaolin powder (MK). The physical properties of MK are briefly presented in Table 3. This material was purchased from the Jahan Dilijan Powder Company.

TABLE 3. Physical properties of metakaolin

Specific weight	Bulk density	pH	wt. %	Particle size
2.5 g	0.6 g/ml	5/2	90%	25.00-99.87 μm
			50%	12.66-15.00 μm
			10%	0.49-0.60 μm

The chemical composition (XRF) of MK is presented in Table 4. The chemical analysis shows that MK is composed of 41% SiO<sub>2</sub>, 17% CaO, 14% LOI, and 11% Al<sub>2</sub>O<sub>3</sub> and small amounts of Fe<sub>2</sub>O<sub>3</sub>, MgO, and K<sub>2</sub>O.

TABLE 4. Chemical composition of metakaolin by XRF analysis [%]

	SiO <sub>2</sub>	Al <sub>2</sub> O <sub>3</sub>	Fe <sub>2</sub> O <sub>3</sub>	CaO	Na <sub>2</sub> O	K <sub>2</sub> O	MgO	TiO <sub>2</sub>	MnO	P <sub>2</sub> O <sub>5</sub>	LOI
MK	41.21	11.163	5.178	17.059	1.173	3.262	4.542	0.533	0.085	0.128	14.23

### Specimen preparation

The specimens were prepared by adding 0, 3, 5, 7, and 9 grams of MK in 100 grams of gypsum powder and then evenly sprinkled in a bowl with 80 ml of water at room temperature within 10 seconds. In accordance with EN ISO 6873, when the gypsum and water come into contact, the mixing timer was started and the bowl was mixed for 50 seconds using a manual mixer.

Finally, the mixtures were poured into a steel mold with dimensions of 5 cm x 5 cm x 5 cm and after 15 minutes, the specimens were removed from the molds. Specimens were produced from each mixture and were named as WS, GM3, GM5, GM7 and GM9, respectively. The details of specimen preparation are presented in Table 5.

TABLE 5. Details of specimen preparation

Specimen	Mixing time	Gypsum weight	Additive weight	wt. % of additive	Amount of water
WS	50 seconds	100 g	0	0	80 ml
GM3	50 seconds	100 g	3 g	2.91%	80 ml
GM5	50 seconds	100 g	5 g	4.76%	80 ml
GM7	50 seconds	100 g	7 g	6.54%	80 ml
GM9	50 seconds	100 g	9 g	8.25%	80 ml

## Specification

### Measurement of mechanical properties

Strength tests of the gypsum composites were conducted according to the ASTM C 109-80 standard. An STM-150 testing machine provided by SANTAM Co. with 15 tons of loading capacity was employed for the mechanical tests. For each type of mortar, the test was repeated 6 times and the reported results are an average of 6 tests.

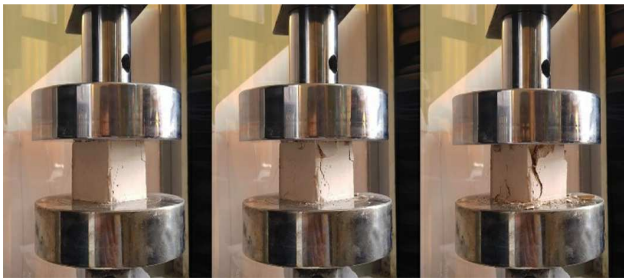


Fig. 1. Specimen failure steps for compression testing

### Setting time measurement

The setting time of the plaster was measured by a Vicat apparatus. The details of specimen preparation are listed in Table 5.

### Physical properties

The percentage of water absorption, porosity, and bulk density were calculated using the Archimedes' method according to ASTM C127, 128 from the equation below. The bulk density was calculated with the following formula:

$$(A) \quad D_b = \frac{W_a}{W_b - W_c} \times 100$$

where:  $W_c$  – immersion weight  $W_b$  – saturation weight  $W_a$  – dry weight

The percentage of open porosity was calculated from the following formula:

$$(B) \quad P_o = \frac{W_b - W_a}{W_b - W_c} \times 100$$

The water absorption percentage was calculated from the following formula:

$$(C) \quad \%W = \frac{W_b - W_a}{W_a} \times 100$$

### XRF microstructure test

To analyze the elements, the XRF test was performed on the specimens by means of a Philips PW3040 X'Pert Pro XRD, Netherlands was used.

### SEM and EDS microstructural analyses

To examine the microstructure of the specimen, it was sputtered with a gold coating and a scanning microscope (SEM, model LEO\_VP 435) with a voltage of 20 kV was used.

## RESULTS AND DISCUSSION

### Density

Table 6 shows the changes in the percentage of porosity, percentage of water absorption, and bulk density of the specimens. According to this table, it is observed that by adding metakaolin up to 6.5%, the apparent porosity is reduced to 37.67%. This change is a 3.83% decrease compared with WS, and with a 8.3% increase in metakaolin, the porosity grew by 4.23% compared with GM7.

TABLE 6. Physical properties of gypsum and specimens with MK additive

Specimen	Bulk density		Water absorption		Porosity	
		SD		SD		SD
WS	1.05 g.ml	0.17	39.44%	4.04	41.50%	3.43
GM3	1.08 g.ml	0.23	36.66%	2.87	39.7%	2.95
GM5	1.06 g.ml	0.29	37.05%	3.82	39.8%	3.37
GM7	1.12 g.ml	0.34	33.57%	5.49	37.67%	4.69
GM9	1.03 g.ml	0.14	40.4%	4.61	41.9%	3.45

### Setting time

Table 7 shows the effect of the initial and final setting time of the gypsum composite specimen. It can be seen that increasing metakaolin reduces the initial and final setting times of gypsum. As a result, the combination of 8.3% metakaolin in the gypsum composite reduces the initial setting of 3.25 min. In other words, adding 8.3% metakaolin to the gypsum composite reduces the initial setting time of the specimen by 45% compared with the WS specimen. In the final set, the time reduction is less, and the final set of the GM9 specimen is 28% less than that of the WS specimen and is premature.

TABLE 7. Initial and final setting times of specimens

Specimen	Initial setting times	Final setting times	Standard deviation (SD)
WS	8.00 min	14.15 min	0.45
GM3	6.10 min	12.30 min	0.50
GM5	5.45 min	11.50 min	0.40
GM7	5.00 min	10.55 min	0.25
GM9	4.35 min	10.20 min	0.30

### Mechanical properties

Figure 2 displays a graph of the results of the 28-day WS and GM3-GM5-GM7-GM9 28-day compressive strength test. In general, the data revealed that the addition of metakaolin increases the compressive strength.

Figure 2 shows that the addition of 2.9% metakaolin raised the compressive strength from 7.44 MPa in the WS specimen to 8.78 MPa. In the GM7 specimen, the compressive strength increased to 10.47 MPa (a 41% increase in strength compared with the WS) and exhibited a dramatic decline by adding metakaolin at the amount of 8.3% by weight of gypsum and reached a value of 7.61 MPa. It is possible that the negative effect of reduced strength in the GM9 specimen is closely related to the lack of an H<sub>2</sub>O ratio to activate the crystals in the gypsum and the unsaturation of calcium hydroxide of the metakaolin. This behavior is also observed in the failure morphology of the specimen. Region c in Figure 3 shows that the gypsum particles in the GM9 specimen are not activated and gypsum and metakaolin enter the final hydration and setting stage before crystal formation. It is also possible to reduce the resistance of GM9 owing to the highest amount of porosity (Table 6) compared to the other specimens, which is because of air bubbles called porosity in the mortar.

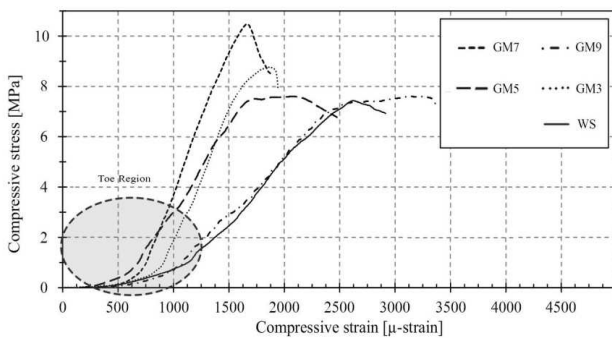


Fig. 2. Stress-strain charts of WS and GM3 GM5 GM7 GM9 specimens (28-day)

Figure 3 displays the SEM micrographs of the GM3, GM7, and WS specimens. As can be seen, GM3 and GM7 exhibit more brittle behavior than the other specimens in their failure level. Figure 3 also shows that in addition to the parallel lines of failure (Region a), in the GM7 specimen leaf cleavage is clearly visible (Region b). This type of fracture morphology indicates the brittleness and high compressive strength of the specimen. The presence of 6.5% metakaolin in the gypsum matrix creates a strong bond. Also, the GM3 specimen has very brittle morphology and is perpendicular to the surface of the fracture plates. The morphological change compared to the plain specimen is due to the presence of metakaolin in the gypsum matrix. These micrographs reveal that the GM3 and GM7 specimens exhibit more brittle behavior compared to the other specimens at their failure level. Moreover, by examining Figure 2, as Gao et al. [32] found, the more stress the specimen bears, the less strain it will withstand.

It is clear that Young's modulus determines the physical parameters and the setting density of gypsum. In addition, the Young's modulus determines the

degree of flexibility of the building materials. The fracture behavior of the mixtures is related to elastic behavior. Figure 4 shows the changes of Young's modulus and fracture strain in the specimens. According to the stress and strain curves, the value of the measured Young's moduli belong to WS, GM9, GM5, GM3, and GM7, respectively, which indicates that the GM7 specimen has the highest Young's modulus (404 MPa) and the GM9 specimen has the lowest Young's modulus (178 MPa) among the specimens. In WS, the fracture strain ratio is 56% higher and the elastic modulus is 52% lower than in GM3. As the amount of metakaolin increases, the fracture strain grows and the Young's modulus decreases, but after raising the amount of metakaolin to 6.5%, the result is reversed. Additionally, by re-increasing the amount of metakaolin to 9%, the Young's modulus reaches a minimum (178 MPa) and the strain of failure reaches a maximum (0.0677%). As mentioned, this behavior is probably owing to the inactivation of the crystals in the gypsum and the unsaturation of the calcium hydroxide and metakaolin. The amount of porosity in the GM9 specimen determined by the Archimedes method has the highest value compared to the other specimens (Table 6).

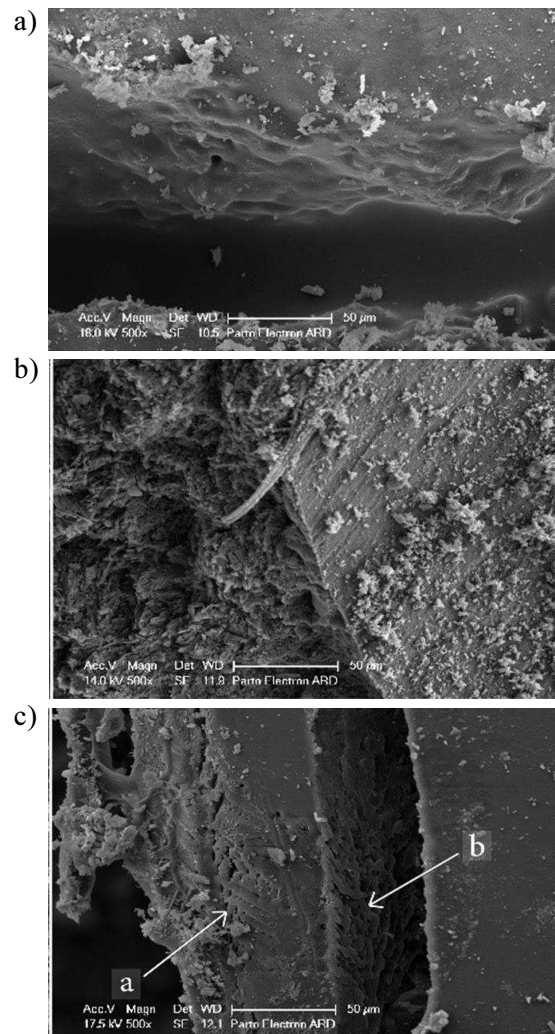


Fig. 3. Structure of: a) gypsum (WS), b) gypsum with 2.9% metakaolin (GM3), c) gypsum with 6.5% metakaolin (GM7)

The TOE region is characterized by a nonlinear stress and strain curve [33]. Figure 4 displays the amount of strain tolerance that the specimens have endured up to this point at the end of the toe. The lower the slope of these two values in Figure 5, the lower the apparent resistance in that specimen [32]. The toe area is shown in Figure 5. The slope of the graphs in the toe region shows the morphology of the onset of cracking. According to the data in Figure 5, the apparent porosity of the specimens can be seen in the WS-GM9 specimens. The toe strain and the apparent porosity are at their maximum value. Therefore, the amount of strain at the beginning of the load in the pressure testing device is directly related to the apparent porosity of the specimens.

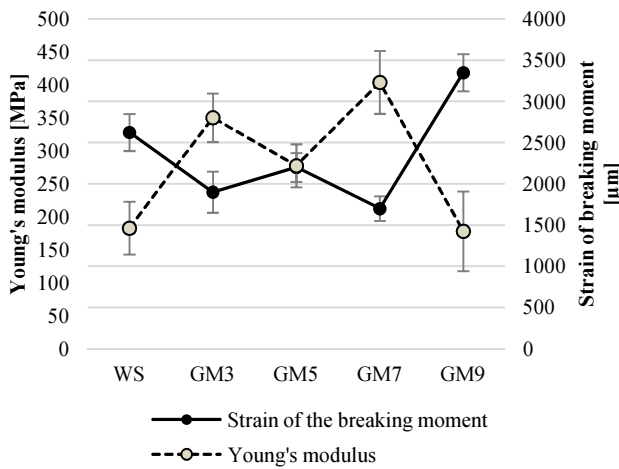


Fig. 4. Changes related to Young's modulus relative to strain of breaking moment in plain gypsum and metakaolin-gypsum composite specimens

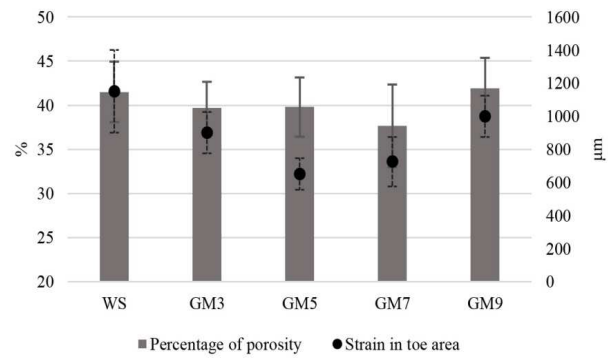


Fig. 5. Comparison of percentage of porosity of specimens with strain in toe area

### SEM and EDS observations

After the gypsum specimens were stored for 7 days, the fracture surface of the gypsum specimens was mounted and then sputtered with gold. Figure 6 presents the SEM and EDS failure level micrographs of specimens. Figure 6a shows no particles due to the lack of complete crystallization of the gypsum particles. The EDS analysis was performed to determine the oxide content of the SEM micrograph regions, as shown in the EDS diagrams. The contents of Ca and S are shown in the diagram in Figure 6a, which indicates the presence of calcium sulfate in the gypsum. As expected, the main elements are calcium, carbon, and oxygen, which confirm the presence of calcite. According to the peak of Si in the diagrams of Figure 6b to 6e, by comparing these data in Figure 7, none of the values of Si of the specimens inside the fractures exceeded 0.07, while the values of Si outside the fractures reach 0.15%.

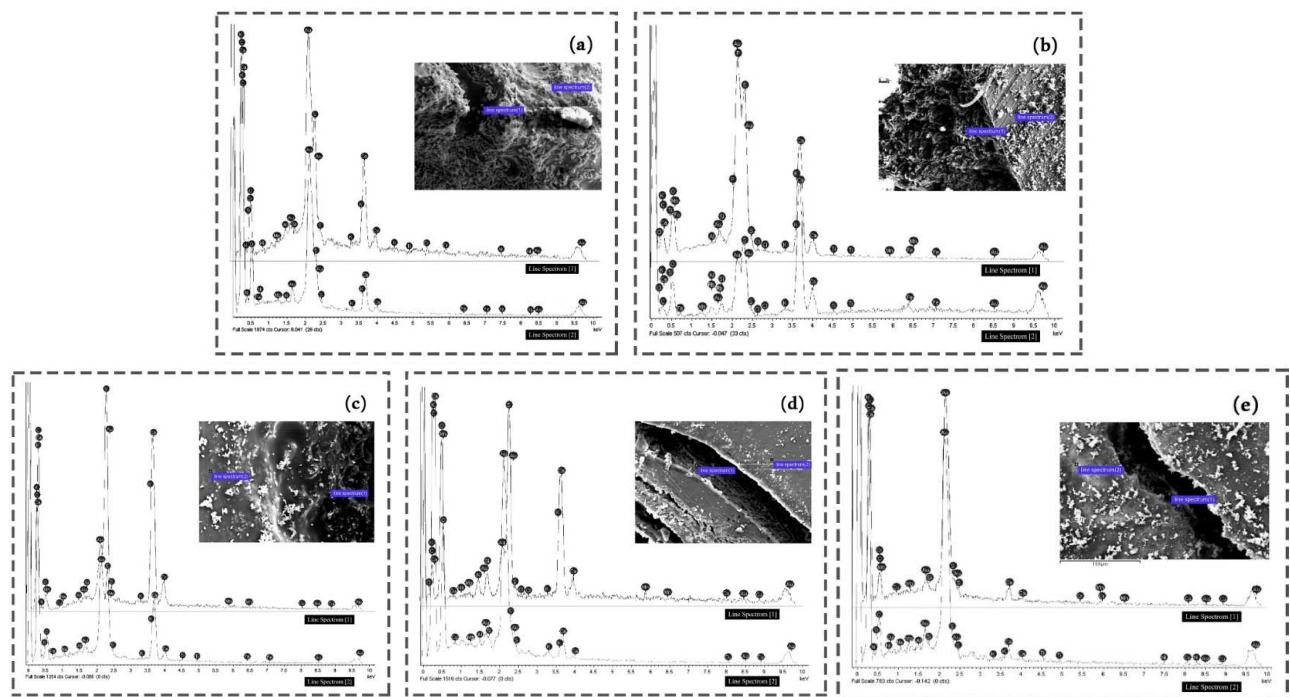


Fig. 6. EDS spectra in crack propagation areas (Segment Line 1) and outside crack (Segment Line 2) – diagram of elements in these areas is shown on the left

Figure 7 shows that the value of Al element inside the fracture surface can reach 0.07 and outside the fracture surface up to 0.085, indicating the presence of more metakaolin outside the fracture surface points. According to Figure 2, the relationship between the compressive strength and the ratio of Al and Si elements inside and outside the fracture surface shows that the presence of metakaolin increased the strength of the specimen. In fact, crack fracture propagation occurred in the absence of metakaolin, i.e. the areas in Figure 6 that contain less Al and Si elements. As can be seen in Figure 6, gypsum particles are present in the specimens presented in Figure 6b to 6e. This probably results from the accelerant setting of the specimens in the presence of metakaolin, in which gypsum crystals were not formed. They had a narrow distribution failure. In addition, there is a significant change in Figure 7 of the GM7 specimen. This difference is clearly seen in Figure 6d and its greater magnification in Figure 3a with the morphology of leaf cleavage. This type of morphology is an example of brittle failure and the high ultimate strength of the specimen. The presence of metakaolin in the gypsum matrix created a strong bond (see Figure 2 for pressure diagrams). This phenomenon is associated with the formation of parallel sliding systems inside, which indicates the presence of MK [34].

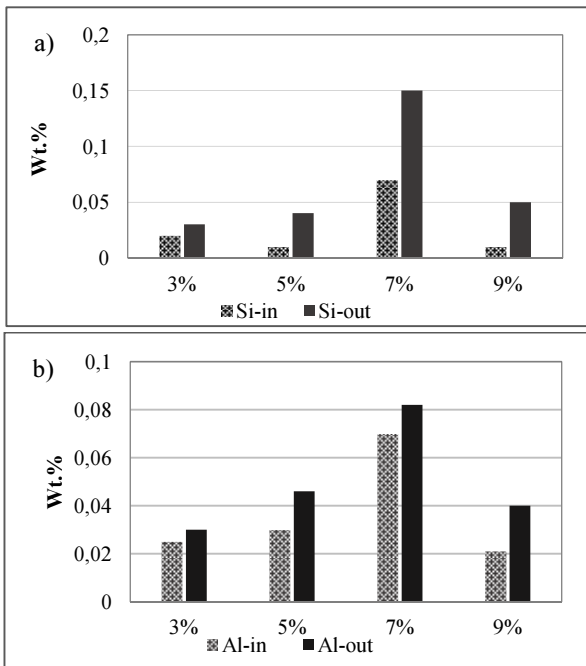


Fig. 7. a) Comparison of silicon levels inside and outside fracture in specimens containing 2.9, 4.8, 6.5, and 8.3% metakaolin, b) Comparison of aluminum values inside and outside fracture in specimens containing 2.9, 4.8, 6.5, and 8.3% metakaolin

## CONCLUSION

In this paper, the effect of metakaolin on the properties of gypsum was investigated and it was shown that metakaolin and its amount affect the hydration process and structure of gypsum. From the experimental study

on metakaolin-gypsum, it was found that the addition of metakaolin to gypsum is a successful solution to strengthen their physical and mechanical properties. Thus, the present research can be concluded as follows:

1. The improvement in the mechanical properties in the metakaolin plaster composites was different due to the presence of additive particles in the interstitial pores of the plaster matrix with the change in the percentage of additive. The results of the EDS-SEM investigations indicate the presence of more Al and Si elements outside the fracture surface. This indicates the presence of more metakaolin outside the fracture surface points.
2. It can be concluded that the presence of metakaolin elements at one point increased the resistance and failure in that area. Although we obtained positive results in mechanical behavior by adding 6.5% metakaolin and it is a good model for further research, these results provide only a partial answer and the decision to optimize the specimen with 6.5% metakaolin compared to the other specimens is a very early decision.
3. Therefore, such gypsum/additive composites can be suitable for building units, boards and panels in various light-weight and high-porosity applications (such as desert buildings or similar climatic conditions).

It is suggested that further studies, including the study of moisture and heat behavior, are needed to decide whether these findings could indicate the optimal concentration of 6.5% metakaolin additive in use.

## Acknowledgements

The authors thank Ms. Mahdieh Fadai, Mr. Ahmad Izadi, Dr. Mahdi Omidi, and Dr. Leyla Adelzade Saadabadi for their help and guidance in conducting the tests. The experimental work was done in the Advanced Materials Laboratory at Najafabad Azad University, where the authors would like to thank the laboratory technician, especially Mr. Chami and Mr. Soheili.

## REFERENCES

- [1] Abidi S., Joliff Y., Favotto C., Impact of perlite, vermiculite and cement on the Young modulus of a plaster composite material: Experimental, analytical and numerical approaches, *Compos. Part B Eng.* 2016, 92, 28-36, DOI: 10.1016/j.compositesb.2016.02.034.
- [2] Doleželová M., Scheinherrová L., Krejsová J., Vimmrová A., Effect of high temperatures on gypsum-based composites, *Constr. Build. Mater.* 2018, 168, April, 82-90, DOI: 10.1016/j.conbuildmat.2018.02.101.
- [3] Medina N.F., Barbero-Barrera M.M., Mechanical and physical enhancement of gypsum composites through a synergic work of polypropylene fiber and recycled isostatic graphite filler, *Constr. Build. Mater.* 2017, 131, January, 165-177, DOI: 10.1016/j.conbuildmat.2016.11.073.
- [4] Singh N.B., Vellmer C., Middendorf B., Effect of carboxylic acids on the morphology, physical characteristics and

- hydration of  $\alpha$ -hemihydrate plaster, *Constr. Build. Mater.* 2005, 12, 4, 337-344, DOI: 10.1016/j.conbuildmat.2010.12.005.
- [5] Bicer A., Kar F., Thermal and mechanical properties of gypsum plaster mixed with expanded polystyrene and tragacanth, *Therm. Sci. Eng. Prog.* 2017, 1, March, 59-65, DOI: 10.1016/j.tsep.2017.02.008.
- [6] Gencil O., del Coz Diaz J.J., Sutcu M., Koksal F., Álvarez Rabanal F.P., Martínez-Barrera G., A novel lightweight gypsum composite with diatomite and polypropylene fibers, *Constr. Build. Mater.* 2016, 113, June, 732-740, DOI: 10.1016/j.conbuildmat.2016.03.125.
- [7] Arikan M., Sobolev K., The optimization of a gypsum-based composite material, *Cem. Concr. Res.* 2002, 32, 11, November, 1725-1728, DOI: 10.1016/S0008-8846(02)00858-X.
- [8] Iucolano F., Caputo D., Leboffe F., Liguori B., Mechanical behavior of plaster reinforced with abaca fibers, *Constr. Build. Mater.* 2015, 99, November, 184-191, DOI: 10.1016/j.conbuildmat.2015.09.020.
- [9] Schug B. et al., A mechanism to explain the creep behavior of gypsum plaster, *Cem. Concr. Res.* 2017, 98, August, 122-129, DOI: 10.1016/j.cemconres.2017.04.012.
- [10] Kretova V., Hezhev T., Mataev T., Hezhev K., Vasily A., Gypsumcementpozzolana composites with application volcanic ash, *Procedia Eng.* 2015, 117, 206-210, DOI: 10.1016/j.proeng.2015.08.142.
- [11] Cotrim H., do Rosario Veiga M., de Brito J., Freixo palace: Rehabilitation of decorative gypsum plasters, *Constr. Build. Mater.* 2008, 22, 1, January 41-49, DOI: 10.1016/j.conbuildmat.2006.05.060.
- [12] Khalil A.A., Tawfik A., Hegazy A.A., Plaster composites modified morphology with enhanced compressive strength and water resistance characteristics, *Constr. Build. Mater.* 2018, 167, 55-64, DOI: 10.1016/j.conbuildmat.2018.01.165.
- [13] Kondratieva N., Barre M., Goutenoire F., Sanytsky M., Study of modified gypsum binder, *Constr. Build. Mater.* 2017, 149, September, 535-542, DOI: 10.1016/j.conbuildmat.2017.05.140.
- [14] Vimmrová A., Keppert M., Svoboda L., Černý R., Lightweight gypsum composites: Design strategies for multifunctionality, *Cement and Concrete Comp.* 2011, 33, 1, 84-89, DOI: 10.1016/j.cemconcomp.2010.09.011.
- [15] Singh M., Garg M., Glass fibre reinforced water-resistant gypsum-based composites, *Cement and Concrete Comp.* 1992, 14, 1, 23-32, DOI: 10.1016/0958-9465(92)90036-U.
- [16] Zhu C., Zhang J., Peng J., Cao W., Liu J., Physical and mechanical properties of gypsum-based composites reinforced with PVA and PP fibers, *Constr. Build. Mater.* 2018, 163, February, 695-705, DOI: 10.1016/j.conbuildmat.2017.12.168.
- [17] Vejmelková E., Koňáková D., Čáchová M., Keppert M., Černý R., Effect of hydrophobization on the properties of lime-metakaolin plasters, *Constr. Build. Mater.* 2012, 37, 556-561, DOI: 10.1016/j.conbuildmat.2012.07.097.
- [18] Mabey M.J., Light-weight, fire-resistant composition and assembly, US Patent, 2017, [Online]. Available: <https://patents.google.com/patent/CA2999580A1/>.
- [19] Koper A., Pralat K., Ciemnicka J., Buczkowska K., Influence of the calcination temperature of synthetic gypsum on the particle size distribution and setting time of modified building materials, *Energies* 2020, 13, 21, DOI: 10.3390/en13215759.
- [20] Chikhi M., Young's modulus and thermophysical performances of bio-sourced materials based on date palm fibers, *Energy Build.* 2016, 129, October, 589-597, DOI: 10.1016/j.enbuild.2016.08.034.
- [21] Tokarev Y., Ginchicki J., Sychugow S., Krutikow W., Jankowlew G., Burianow A., Senkow S., Modification of gypsum binders by using carbon nanotubes and mineral additives, *Procedia Eng.* 2017, 172, 1161-1168, DOI: 10.1016/j.proeng.2017.02.135.
- [22] Noushini A., Hastings M., Castel A., Aslani F., Mechanical and flexural performance of synthetic fibre reinforced geopolymer concrete, *Constr. Build. Mater.* 2018, 186, October, 454-475, DOI: 10.1016/j.conbuildmat.2018.07.110.
- [23] Kalaiyarrasi A.R.R., Priyadharshini S.P., Fibre reinforced metakaolin geopolymer composite, *Int. J. Recent Sci. Res.* 2018, 9, 8(A), 28303-28305, DOI: 10.24327/ijrsr.2018.0908.2434.
- [24] Arsalan Mohammad Ali Akram, Aijaz Ali, A study on nylon fibre reinforced concrete by partial replacement of cement with metakaolin: a literature review, *Int. Res. J. Eng. Technol.* 2018, e-ISSN: 2395-0056.
- [25] Pundir A., Garg M., Singh R., Evaluation of properties of gypsum plaster-superplasticizer blends of improved performance, *J. Build. Eng.* 2015, 4, December, 223-230, DOI: 10.1016/j.jobe.2015.09.012.
- [26] Ozerkan N.G., Ahsan B., Mansour S., Iyengar S.R., Mechanical performance and durability of treated palm fiber reinforced mortars, *Int. J. Sustain. Built Environ.* 2013, 2, 2, December, 131-142, DOI: 10.1016/j.ijsbe.2014.04.002.
- [27] Mohandes J.A., Sangghaleh A., Nazari A., Pourjavad N., Analytical modeling of strength in randomly oriented PP and PPTA short fiber reinforced gypsum composites, *Comp. Mater. Sci.* 2011, 50, 5, 1619-1624, DOI: 10.1016/j.commatsci.2010.12.020.
- [28] Tabatabai H., Janbaz M., Nabizadeh A., Mechanical and thermo-gravimetric properties of unsaturated polyester resin blended with FGD gypsum, *Constr. Build. Mater.* 2018, 163, February 438-445, DOI: 10.1016/j.conbuildmat.2017.12.041.
- [29] Palou M., Kuzielová E., Žemlička M., Novotný R., Másilko J., The effect of metakaolin upon the formation of ettringite in metakaolin-lime-gypsum ternary systems, *J. Therm. Anal. Calorim.* 2018, 133, 1, 77-86, DOI: 10.1007/s10973-017-6885-0.
- [30] McLellan B.C., Williams R.P., Lay J., Van Riessen A., Corder G.D., Costs and carbon emissions for geopolymer pastes in comparison to ordinary portland cement, *J. Clean. Prod.* 2011, 19, 9-10, 1080-1090, DOI: 10.1016/j.jclepro.2011.02.010.
- [31] Davidovits J., False values on CO<sub>2</sub> emission for geopolymer cement/concrete, [in:] *Scientific Papers, Geopolymer Inst. Libr. Tech. Pap.* 2015, 24, 1-9.
- [32] Gao H.T., Liu X.H., Zhang S.J., Qi J.L., Synergistic effect of glass fibre and Al powder on the mechanical properties of glass-ceramics, *Ceram. Int.* 2018, 44, 13, 15167-15175, DOI: 10.1016/j.ceramint.2018.05.155.
- [33] Robi K., Jakob N., Matevz K., Matjaz V., The Physiology of sports injuries and repair processes, *Curr. Issues Sport. Exerc. Med.* 2013, DOI: 10.5772/54234.
- [34] Jiang S., Guo S., Huang Y., Ning Z., Xue P., Ru W., Zhang J., Sun J., In situ study of the shear band features of a CuZr-based bulk metallic glass composite, *Intermetallics* 2019, 112, June, 106523, DOI: 10.1016/j.intermet.2019.106523.